POLITECNICO DI TORINO
Repository ISTITUZIONALE

Multimodal T2w and DWI Prostate Gland Automated Registration

(Article begins on next page)

21 May 2024

Multimodal T2w and DWI Prostate Gland Automated Registration

Bruno De Santi, Massimo Salvi, Valentina Giannini, Kristen M. Meiburger, Nicola Michielli, Silvia Seoni, Daniele Regge, Filippo Molinari

Abstract— **Multiparametric magnetic resonance imaging (mpMRI) is emerging as a promising tool in the clinical pathway of prostate cancer (PCa). The registration between a structural and a functional imaging modality, such as T2-weighted (T2w) and diffusion-weighted imaging (DWI) is fundamental in the development of a mpMRI-based computer aided diagnosis (CAD) system for PCa. Here, we propose an automated method to register the prostate gland in T2w and DWI image sequences by a landmark-based affine registration and a non-parametric diffeomorphic registration. An expert operator manually segmented the prostate gland in both modalities on a dataset of 20 patients. Target registration error and Jaccard index, which measures the overlap between masks, were evaluated pre- and post- registration resulting in an improvement of 44% and 21%, respectively. In the future, the proposed method could be useful in the framework of a CAD system for PCa detection and characterization in mpMRI.**

I. INTRODUCTION

In European Union, prostate cancer (PCa) is the most common cancer in men and about 450'000 cases are estimated for 2018 [1]. Currently, the standard technique to diagnose PCa is transrectal ultrasound (TRUS) guided core biopsy which is invasive and with relatively low diagnostic accuracy [2].

In the last decade, multiparametric-Magnetic Resonance Imaging (mpMRI) has had an increasing role in the PCa clinical pathway. MpMRI is defined as the integration of structural MRI, T1-weighted (T1w) or T2-weighted (T2w) volumes, with functional imaging, such as diffusion-weighted imaging (DWI) or dynamic contrast-enhanced imaging. Previous studies showed that T2w imaging improves the detection of PCa especially in the peripheral zone [2] and DWI images have proven to be useful to characterize PCa and tumor aggressiveness [3].

The integration of multiple modalities in a single system, specifically DWI and T2w imaging, increases the accuracy in PCa detection and characterization, when compared to a unique MRI modality or to TRUS-guided biopsy alone [2].

However, the development of a mpMRI-based computer-aided diagnosis (CAD) system for PCa strongly requires a robust and accurate method to register images from different modalities, which is not a trivial task due to: i) different appearances of the prostate gland (PG); ii) presence of physiological motion; iii) nonlinear geometric distortions caused by susceptibility artifacts and echo-planar imaging (EPI) sequence, which is the standard sequence used to acquire DWI images [4].

In most of the current CAD systems, the registration is semi-automatic where the operator manually places control points in the images resulting in a high inter-operator variability. Automatic multimodal registration algorithms mainly consist of nonrigid transformations where the moving image is deformed iteratively to maximize a similarity criterion such as mutual information, mean squared error or cross correlation. In a previous study, five state-of-the-art nonrigid registration algorithms were tested on a dataset of 20 patients with cancerous lesions or cysts, acquired with a 3T MRI Scanner [4]. However, the results of these methods are strongly dependent on the initial deformation between the images, hence, the parameter selection could be hard if a good initial transformation is not provided. An automatic method was proposed to align the PG in T2w and DWI images [5]. The method was based on a deformation field decreasing along the phase encode direction, linearly with the distance from the endorectal coil. However, such method presents two major limitations: i) the same transformation is applied for each slice of the PG volume, which may lead to an overestimation of the deformation in the slices far from the coil center, ii) the decreasing rate of the vertical displacement is chosen by maximizing the registration accuracy on a training set which may not be representative of every prostate.

In this study, we propose an innovative and automatic algorithm to align the PG in DWI and T2w image sequences. The methodology is able to: i) extract a region-of-interest enclosing the PG, ii) correct physiological motion deformation by estimating an affine transformation and iii) correct nonlinear geometric distortions using the diffeomorphic demons registration algorithm.

II. METHODS

A. Image Dataset

Twenty patients were enrolled in this study: age, 63 ± 5 y.o. and prostate volume, 35.3 ± 7.2 cm^3. For each patient, peripheral zone PCa was histologically confirmed after radical prostatectomy. For each patient, a T2w and a DWI (b-value = 0 and 1000 s/mm^2) axial volume were acquired using the same acquisition parameters adopted in a previous work [5]. The field of view was 160 x 160 mm for both modalities and voxel size was 0.3125 x 0.3125 x 3 mm in T2w volumes and 0.625 x 0.625 x 3 mm in DWI volumes. A 1.5 T scanner (Signa Excite HD, GE Healthcare, Milwaukee, Wisconsin, USA) with a four-channel phased-array coil and an endorectal coil (Medrad, Indianola, Pa) was used. The local ethics committee approved the study.

B. De Santi, M. Salvi, K.M. Meiburger, N. Michielli, S. Seoni and F. Molinari are with the PoliTo BIO^Med Lab, Department of Electronics and Telecommunications, Politecnico di Torino, Turin, Italy. (corresponding author to provide e-mail: bruno.desanti@polito.it).

V. Giannini and D. Regge are with the Candiolo Cancer Institute, FPO-IRCCS, Candiolo, Turin, Italy.

Figure 1. Automatic ROI extraction in a DWI (top panels) and a T2w (bottom panels) slice. *(A,B) Original images; (C,D) Median smoothing and contrast-enhancement; (E) DWI binary mask obtained with the object-detection; (F) Otsu thresholding in T2w; (G) antero-posterior (green points) and medio-lateral (yellow points) bounds estimation; (H) EC profile (red line) identification; (I,L) final ROI (solid line) extraction, the dashed lines represent the rectangles obtained using the estimated bounds.*
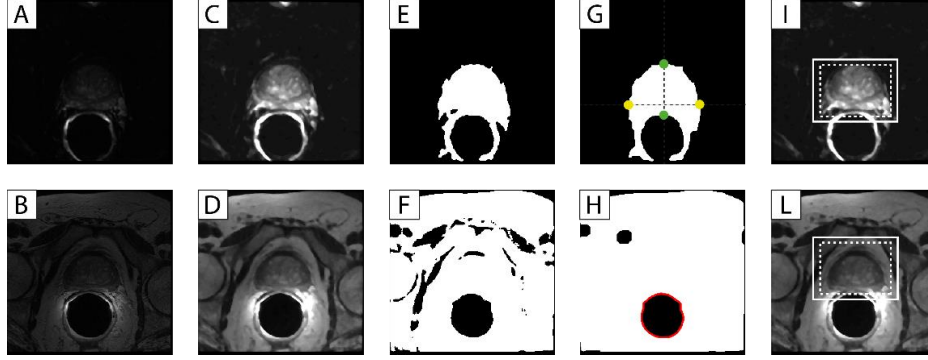
An expert operator (D.R. with 9 years of experience in MRI prostate examination) contoured the PG in each volume in both modalities using the open-source software 3DSlicer. A set (approximately 30 points per PG) of landmarks was defined by the same operator. These landmarks were visible in both modalities and positioned in anatomical points, as suggested in [4].

B. Automatic Registration Algorithm

The proposed algorithm automatically aligns the PG in DWI and T2w images. The algorithm involves four major steps: i) region-of-interest extraction; ii) key points extraction and key points matching; iii) affine transformation estimation and iv) non-parametric diffeomorphic registration. Since the voxel resolution along z is significantly lower compared to the in-plane resolution, the first two steps are designed to work on 2D. Following paragraphs will describe in more detail each processing step.

First, a 2-D median filtering with a window size equal to 3 mm x 3 mm is applied in the DWI (b-value = 0 s/mm^2) image (Fig. 1A) followed by a contrast enhancement saturating the bottom 1% and the top 1% of all pixel values (Fig. 1C). Next, a binary mask including the prostate and the endorectal coil artifact in the DWI image is obtained using an object-based detection algorithm which was adapted to these images (Fig. 1E) [6]. Morphological closing (structural element: disk, radius 3 mm) was performed to remove spurious holes in the mask. Antero-posterior and medio-lateral bounds of the PG are estimated by scanning the binary mask with a vertical and a horizontal line passing by the mask centroid (Fig. 1G). A rectangle passing by the estimated bounds is drawn, and a ROI is obtained by rescaling this rectangle with a scaling factor equal to 1.2 to ensure that the ROI will cover the entire gland (Fig. 1I). Regarding the T2w image (Fig. 1B), as first step the image is resized to match the DWI image size. Then, the same median filtering and contrast enhancement used in DWI is performed (Fig. 1D). The image is Otsu thresholded to obtain a binary mask in which the rectum is a black circle (Fig. 1F). To identify the rectum, the Otsu binary mask is morphologically closed (structural element: disk, radius 3 mm) and the dark object with the largest area is defined to

be the rectum (Fig. 1H). Next, the rectangle passing by the estimated bounds in DWI is positioned in the T2w image so that the lower bound of the ROI coincides with the upper bound of the rectum. The rectangle is then 120% rescaled to obtain a ROI including the entire PG (Fig. 1L).

At this point, both images (DWI and T2w) are cropped in correspondence to their ROI, as shown in Fig.2A and 2B, and filtered with a multiscale Laplacian-of-Gaussian (LoG) filter. This filter is commonly used in image processing to enhance blob-like structures. As the standard deviation of the LoG kernel (σ) governs the size of the blobs detected, we performed LoG filtering at five different values of σ (4, 6, 8, 10 and 12) using a kernel size of $2\sigma \times 2\sigma$ and then sum up the four output images to obtain a unique image. As observable in Fig. 2C and 2D, the application of this filter highlights similar structures within the two images, neglecting the different fine-textures peculiar of the two sequence modalities.

Scale-invariant feature transform (SIFT) algorithm is then used to extract key points in the filtered images [7]. This computer vision algorithm involves multiple steps: i) detecting candidate key points at different scales; ii) discarding points with low contrast with respect to the neighbourhood or localized along an edge; iii) for each point, computing a descriptor which is a 128-element vector derived from the local image gradient magnitude and orientation. Fig. 2E and 2F show the key points extracted respectively in the DWI and the T2w image. Given a key point in the DWI image, represented by its SIFT descriptor, key points matching means finding the best partner point in the T2w image. This can be addressed as a linear assignment problem. In our application, the assignment cost is defined as the Euclidean distance between the two descriptors and Kuhn-Munkres algorithm, also known as Hungarian algorithm, is used as it provides an optimal solution to the linear assignment problem in polynomial runtime complexity. Under the assumption that geometric distortions occur mainly along the phase encode direction [5], that corresponds to the antero-posterior direction, matching key points which are distant more than 3 mm along the

Figure 2. Key points extraction and matching in a DWI (top panels) and a T2w (bottom panels) slice. *(A,B) cropped images; (C,D) Multiscale LoG filtering output images; (E,F) SIFT key points (blue points) extracted; (G,H) Key points matching, red line represent a discarded match where the matching points have a difference higher than 3 mm between the medio-lateral coordinates while green lines represent good matches.*
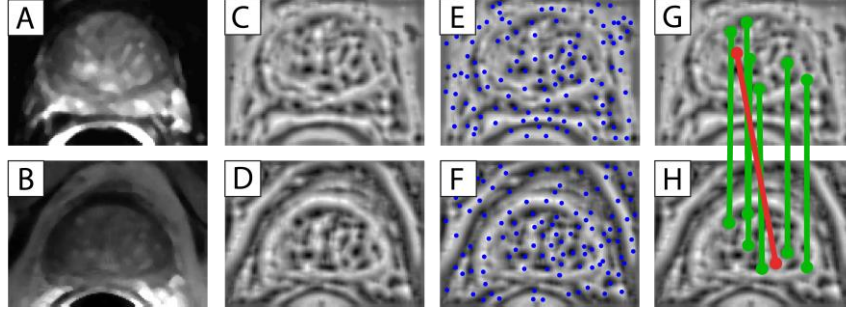
mediolateral direction are discarded, as illustrated in Fig. 2G and 2H.

Then, every pair of matching points obtained throughout the entire volume is used to estimate a 3D affine transformation between the two volumes (DWI and T2w) by linear least squares fitting. This step is used to correct for physiological motion, further, to provide an accurate initialization for the non-parametric diffeomorphic registration which mainly corrects EPI-specific geometric distortions.

Finally, the DWI affine corrected volume is registered to the T2w volume using the demons deformable registration algorithm. The basic idea of this algorithm is to apply the diffusing models to the image matching problem by considering the contours of an object in an image as semi-permeable membranes and deforming, in an iterative scheme, the second image to diffuse through these membranes. Before applying the nonrigid registration, volumes are cropped considering the largest ROI obtained throughout the slices and images are filtered with the multiscale LoG filtering. Mutual information is used as similarity measure, the number of iterations is 300.

B. Performance metrics and statistical analysis

Target registration error was evaluated by computing the mean euclidean distance between the anatomical landmarks defined by the expert in T2w and in DWI before and after the automated registration.

Mutual information (MI) values of the T2w and the DWI volumes before and after the registration were computed within a volume-of-interest defined by an expert. MI is a measure of the amount of information that two images share [8]. This metric is assumed to be higher when the images are aligned. This is defined as:

$$MI(A, B) = H(A) + H(B) - H(A, B) \qquad (1)$$

where $H(A)$ and $H(B)$ are the marginal entropies of image A and image B respectively and $H(A,B)$ is their joint entropy.

Further, we performed a similarity analysis between the 3D masks manually drawn by the operator in DWI and in T2w pre- and post- registration. The Jaccard index (JI) was used to measure the overlap between two masks computed as the intersection over union of the two masks.

For each metric, two-tailed paired sample t-test was performed to test whether the mean difference between the metric values pre- and post- registration was zero. The significance level was set to 0.05.

The algorithm was also tested separately in the slices belonging to the base (defined as the cranial 1/3 part of the prostate volume) and apex (caudal 1/3 part of the prostate volume) of the PG to evaluate the robustness of the methodology in the different gland zones.

III. RESULTS

The algorithm took less than 24 minutes to process the entire image dataset (20 patients), thus the average computational time per patient was approximately 72 seconds on a Intel(R) Core(TM) i7 with 2.2 GHz, 16 GB RAM memory.

Fig. 3 shows registration results for three representative images of base, mid-gland and apex of the prostate.

Table 1 reports mean and standard deviation values of TRE, MI and JI pre- and post- registration at different gland zones. Paired t-test shows the presence of a statistically significant improvement of all the three metrics and for every gland zone (p < 0.001) with the automatic registration.

Table 1. *Mean (standard deviation) values of target registration error (TRE), mutual information (MI) and Jaccard index (JI) pre- and post-automatic registration for apex, base and whole prostate gland (PG). Δ% represents the patient-wise mean percentage of increasing/decreasing of the metric.*

Metric	Zone	Pre-registration	Post-registration	Δ%
TRE (mm)	Base	3.38 (1.25)	2.02 (1.11)	-36
	Apex	2.40 (0.97)	1.75 (0.88)	-29
	PG	3.12 (1.19)	1.69 (1.18)	-44
MI	Base	0.56 (0.28)	0.63 (0.19)	11
	Apex	0.64 (0.22)	0.70 (0.14)	8
	PG	0.66 (0.20)	0.71 (0.18)	9
JI	Base	0.66 (0.14)	0.76 (0.11)	20
	Apex	0.71 (0.13)	0.79 (0.12)	14
	PG	0.68 (0.11)	0.81 (0.06)	21

Figure 3. Qualitative automatic registration results for different prostate zones. *Left column panels represent the fused images pre-registration while right column ones are the fused images post-registration. (A,B) base slice; (C,D) mid-gland slice; (E,F) apex slice. White and green points represent the axial projections of some anatomical points annotated by the expert in the DWI and in the T2w image, respectively.*
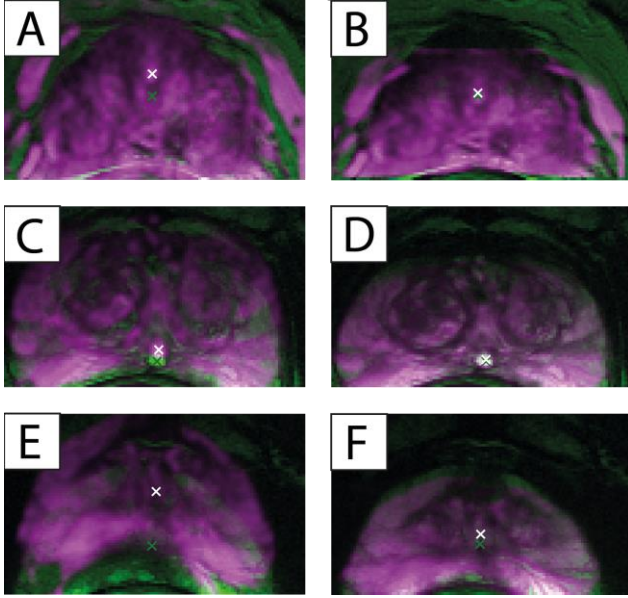
IV. DISCUSSION AND CONCLUSIONS

In this study, an automatic algorithm for prostate gland (PG) registration in DWI and T2w images was proposed. Most of the current registration methods are manual or semi-automatic leading to high inter-operator and intra-operator variability.

In our previous work, we used as transformation model a piecewise linear with the deformation decaying linearly along the phase-encode direction. However, the decay parameter was chosen on a training set, thus leading to poor reproducibility and generalization. The method proposed in this study yields a mean percentage of JI increase equal to 21% compared to 17% obtained in [5]. We believe that the increased performances are due to the combination of the two registration steps (affine and diffeomorphic) which gives more adaptability and robustness to the methodology. The proposed method was compared to five state-of-the-art registration algorithms [4]. Our registration results, in terms of TRE and computational time, are comparable or better than the results of four of these algorithms (mean TRE from 1.53 to 2.05 mm, average computational time per patient from 36 to 216 s), while the "fast elastic image registration" method yielded the most accurate alignment (mean TRE: 1.07 mm, average computational time per patient: 11 s). However, the mean TRE computed before registration was 2.21 mm (compared to 3.12 mm in our dataset), further, the authors tested the algorithms on an image set acquired with a 3T MRI scanner, which results in a better signal-to-noise ratio, compared to the 1.5T scanner used in this study.

In every patient, the automatic registration improved the overlap between the masks and the distance between the anatomical landmarks annotated by the expert. In the same way, the affine transformation estimated through the SIFT key points produced an improvement of the alignment between the volumes (ΔTRE: -40%, ΔMI: 3%, ΔJI: 20%).

However, the methodology presents some limitations. In the prostate's apex, the performances of the proposed registration algorithm are lower than in the whole PG (ΔTRE: -29% vs -44%, ΔMI: 8% vs 9%, ΔJI: 14% vs 21%). Indeed, being the PG smaller in apex slices, the number of SIFT key points extracted is often lower thus the estimation of the affine transformation produces worse results in this zone.

In the future, the algorithm will be improved by implementing a new strategy for the apical portion of the gland. Further, the methodology will be validated on a larger dataset with multiple configurations of acquisition parameters to assess its robustness to different image characteristics.

In conclusion, the proposed method could be a powerful tool to enable the development of CAD systems for PCa detection and characterization in mpMRI.

REFERENCES

[1] J. Ferlay *et al.*, "Cancer incidence and mortality patterns in Europe: Estimates for 40 countries and 25 major cancers in 2018," *Eur. J. Cancer*, 2018.

[2] L. C. Brown *et al.*, "Multiparametric MRI to improve detection of prostate cancer compared with transrectal ultrasound-guided prostate biopsy alone: the PROMIS study," *Health Technol. Assess. (Rockv).*, vol. 22, no. 39, pp. 1–176, Jul. 2018.

[3] T. Hambrock *et al.*, "Prospective assessment of prostate cancer aggressiveness using 3-T diffusion-weighted magnetic resonance imaging-guided biopsies versus a systematic 10-core transrectal ultrasound prostate biopsy cohort," *Eur. Urol.*, vol. 61, no. 1, pp. 177–184, 2012.

[4] C. Buerger *et al.*, "Comparing nonrigid registration techniques for motion corrected MR prostate diffusion imaging," *Med. Phys.*, vol. 42, no. 1, pp. 69–80, Dec. 2015.

[5] V. Giannini *et al.*, "A Novel and Fully Automated Registration Method for Prostate Cancer Detection Using Multiparametric Magnetic Resonance Imaging," *J. Med. Imaging Heal. Informatics*, vol. 5, no. 6, pp. 1171–1182, Nov. 2015.

[6] M. Salvi and F. Molinari, "Multi-tissue and multi-scale approach for nuclei segmentation in H&E stained images," *Biomed. Eng. Online*, vol. 17, no. 1, p. 89, Dec. 2018.

[7] D. G. Lowe, "Distinctive image features from scale-invariant keypoints," *Int. J. Comput. Vis.*, vol. 60, no. 2, pp. 91–110, Nov. 2004.

[8] H. W. Kuhn, "The Hungarian method for the assignment problem," *50 Years Integer Program. 1958-2008 From Early Years to State-of-the-Art*, vol. 2, no. 1–2, pp. 29–47, Mar. 2010.